

## FINDING UNIQUE THERMAL EMISSION SPECTRA OF THE ASTEROID BENNU THROUGH MACHINE

LEARNING MODEL APPLICATIONS. L. B. Breitenfeld<sup>1</sup>, A. D. Rogers<sup>1</sup>, T. D. Glotch<sup>1</sup>, V. E. Hamilton<sup>2</sup>, P. R.

Christensen<sup>3</sup>, and D. S. Lauretta<sup>4</sup>, <sup>1</sup>Dept. of Geosciences, Stony Brook University, Stony Brook, NY,

laura.breitenfeld@stonybrook.edu, <sup>2</sup>Dept. of Space Science, Southwest Research Institute, Boulder, CO, <sup>3</sup>School of Earth and Space Exploration, Arizona State University, Tempe, AZ, <sup>4</sup>Lunar and Planetary Laboratory, University of Arizona, Tucson, AZ.

**Introduction:** Bennu, the target of the OSIRIS-REx mission, is a near-Earth asteroid with a composition analogous to type-1 CI and/or CM chondrites [1]. These primitive chondritic meteorites record early Solar System processes such as aqueous alteration. Asteroids like Bennu provide important information about the building blocks of the early Solar System, and therefore the analysis of remote sensing data for mineralogical characterization is advantageous. Here we focus on applying mid-infrared (MIR) machine learning models to OSIRIS-REx Thermal Emission Spectrometer (OTES) data to identify potential spatial variations in mineral abundance across Bennu.

**Background:** Phyllosilicate (e.g., 440  $\text{cm}^{-1}$ ) and magnetite (555, 340  $\text{cm}^{-1}$ ) features are apparent in OTES spectra of Bennu [1]. A broad bowl-shaped feature ( $\sim 1100\text{--}650$   $\text{cm}^{-1}$ ) corresponding to the silicate stretching region is also present. The emissivity maximum around 528  $\text{cm}^{-1}$  is consistent with high phyllosilicate ( $>78$  vol%) and low olivine ( $<10$  vol%) content [2]. Carbonates [3] and rare pyroxene [4] have been detected by other OSIRIS-REx instruments.

Volumetric mineral abundances of Bennu's OTES global average are predicted by machine learning models to be 78% phyllosilicate, 9% olivine, 11% carbonates, and 6% magnetite [5]. Additionally, there is no evidence for major compositional variation on Bennu [2]. Using machine learning, here we investigate subtle compositional variations on the asteroid by applying models to individual OTES spectra.

**Methods:** This study builds on previous work [5] focused on the development of machine learning MIR models for the prediction of modal mineralogy of the asteroid Bennu. The collection of the spectral dataset and the establishment of partial least squares (PLS) machine learning coefficients are detailed in [5]. Instead of applying the PLS models to average OTES spectra as in [5], here we apply the models to individual OTES spectra. This change requires the reduction of PLS coefficients from 1500–310  $\text{cm}^{-1}$  to 1200–310  $\text{cm}^{-1}$  because of wavelength-dependent noise in individual OTES spectra.

After the application of the models, we isolate unique OTES spectra through PLS mineral predictions. We confirm that PLS prediction values are linked to spectral shape through Spectral Angle Mapper (SAM) [6]. And lastly, we investigate the locations of the OTES spectra of interest on Bennu.

**Results:** Our PLS models can predict phyllosilicate, olivine, carbonate, pyroxene, and magnetite abundances [5]. Here, we present analysis of the Mg-rich (antigorite) and Fe-rich (cronstedtite) serpentine predictions (Fig. 1) from the OSIRIS-REx Baseball Diamond 1 (BBD1) OTES dataset, consisting of 4,703 spectra (phase angles  $\sim 5\text{--}10^\circ$ ). We selected spectra with emission angles  $<55^\circ$ , maximum brightness temperatures  $>304$  K, and quality flags ranging from 0–2.

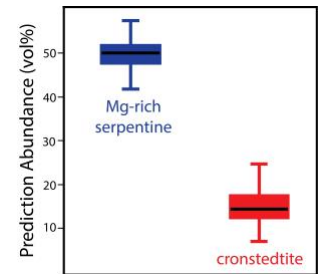


**Fig. 1.** Box-and-whisker plot of PLS serpentine predictions from the BBD1 dataset.

We isolated OTES spectra with high and low prediction values for Mg-rich serpentine and cronstedtite. BBD1 OTES averages of spectra with low (1<sup>st</sup> percentile) and high (99<sup>th</sup> percentile) PLS predictions of Mg-rich serpentine and cronstedtite are shown in Fig. 2. For both Mg-rich serpentine and cronstedtite, there are differences between the 1<sup>st</sup> and

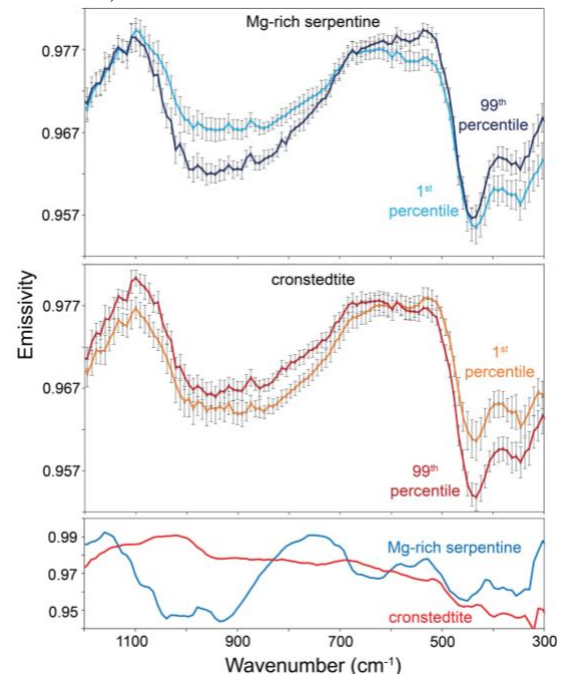


**Fig. 2.** Average BBD1 OTES spectra of the 1<sup>st</sup> and 99<sup>th</sup> percentile PLS predictions of Mg-rich serpentine (top) and cronstedtite (middle), with the standard deviations displayed. For comparison to laboratory spectra, we provide simulated asteroid environment MIR spectra of 50% coarse/50% fine Mg-rich serpentine and cronstedtite (bottom) [5].

99<sup>th</sup> percentile averages in feature shape and/ or depth of the broad bowl-shaped feature ( $\sim 1100\text{--}650\text{ cm}^{-1}$ ) and the  $440\text{ cm}^{-1}$  band.

Unlike other spectral modeling techniques, PLS cannot produce modeled spectra to directly compare to OTEs spectra. Therefore, we use SAM to check that spectral shape is linked to spectra with low or high PLS prediction abundances. We observe the expected trend of low SAM scores (best matches) associated with low prediction values for the 1<sup>st</sup> percentile averages and low SAM scores associated with high prediction values for the 99<sup>th</sup> percentile averages.

Many of the individual OTEs spectra with predictions of low Mg-rich serpentine also were predicted to have high cronstedtite content. We observe that the locations of the spectra with low Mg-rich serpentine and the spectra with high cronstedtite are concentrated in the equatorial region of Bennu (Fig. 3). There is also a band of spectral measurements with low Mg-rich serpentine at the northern mid-latitudes.

**Conclusions and Implications:** We observe spectral variability within the OTEs BBD1 dataset. There are also distinctions between the unique BBD1 spectra (Fig. 2) and the T1 and T2 OTEs spectral types identified by [2]. For example, the cronstedtite 99<sup>th</sup> percentile and Mg-rich serpentine 1<sup>st</sup> percentile averages have shallower  $\sim 1100\text{--}650\text{ cm}^{-1}$  features (with shorter wavelength band minima) and deeper  $440\text{ cm}^{-1}$  absorptions compared with the T1 and T2 spectra. However, our analysis examines BBD1 data instead of the Equatorial Station 3 (EQ3) dataset as in [2]. Therefore, we will expand our analysis to the EQ3 dataset in the future.

Many BBD1 OTEs spectra with predictions of high cronstedtite content have predictions of low Mg-rich serpentine content and are located primarily in the equatorial region. In the OTEs EQ3 dataset, this region

coincides with predominantly T1 spectra that are interpreted as coarse to rocky materials [2]. Our PLS predictions indicate that composition influences spectral shape. Yet previously, particle size was primarily attributed to spectral variability [2]. The dependence of these two factors on one another remains unclear and isolating their effects is complex.

There are many reasons why particle size and compositional heterogeneity could exist on the surface of Bennu. The roles of sorting and alteration must be considered. More specifically, mass movement towards the equator of Bennu [7] could contribute to OTEs spectral variability between the equatorial region and the middle latitudes. The greater abundance of Fe-phyllosilicates (cronstedtite) in the equatorial region may indicate a lower degree of aqueous alteration [8,9] compared to the average surface of Bennu. Evaluating the degree of aqueous alteration can also be accomplished through other quantitative mineralogical markers, and therefore we will reassess this interpretation as more analyses are completed for the other mineral groups.

**Acknowledgments:** This work was supported by the NASA OSIRIS-REx Participating Scientist program under a grant made to T. D. Glotch and A. D. Rogers. This material is based upon work supported by NASA under Contract NNM10AA11C issued through the New Frontiers Program. We are grateful to the OSIRIS-REx Team for making the encounter with Bennu possible.

**References:** [1] Hamilton, V. E. et al. (2019) *Nat. Astron.*, 3, 332. [2] Hamilton, V. E. et al. (2021) *A&A*, 650, A120. [3] Kaplan, H. H. et al. (2020) *Science*, 370, eabc3557. [4] DellaGiustina D. N., Kaplan H. H. et al. (2021) *Nat. Astron.*, 5, 31–38. [5] Breitenfeld, L. B. et al. (2021) *JGR Planets*, 126, e2021JE007035. [6] Kruse, F. A. et al. (1993) *RSE*, 44, 145-163. [7] Jawin, E. R. et al. (2020) *JGR Planets*, 125, e2020JE006475. [8] Browning, L. B. et al. (1996) *GCA*, 60, 2621-2633. [9] Howard, K. T. et al. (2009) *GCA*, 73, 4576-4589.

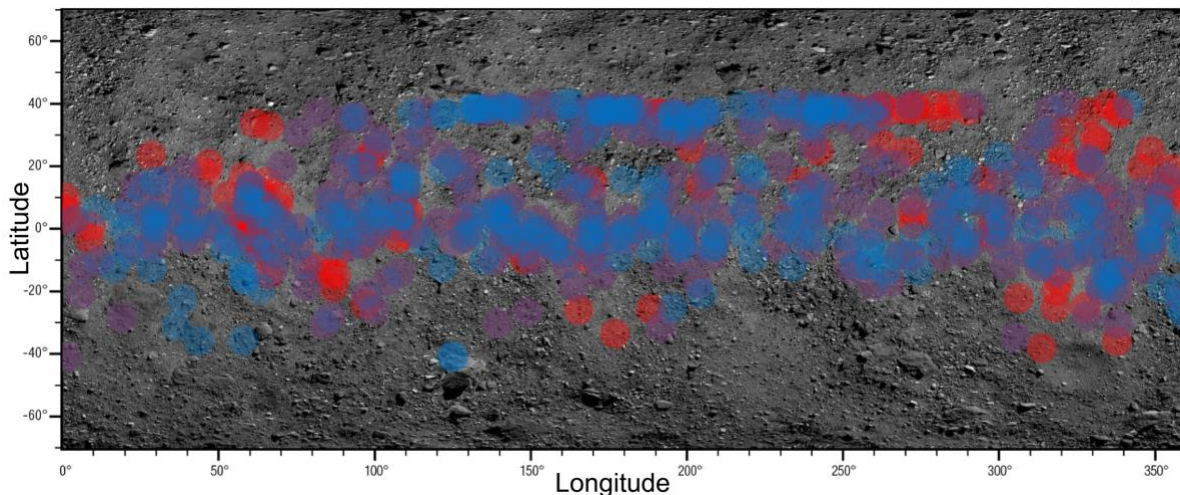


**Fig. 3.** Center positions of OTEs spots with predictions of high cronstedtite content (red) and low Mg-rich serpentine content (blue), or both (purple) based on low SAM scores (best matches). The plotted OTEs spots reflect their center positions but not individual spot shapes that are not necessarily circular.